Context-dependent coordination of movement in *Tribolium castaneum* larvae

Authors

Bella Xu Ying[1,2,3] zxy1@st-andrews.ac.uk
Maarten Frans Zwart[1,2,3]* mfz@st-andrews.ac.uk
Stefan Robert Pulver[1,2,3]* sp96@st-andrews.ac.uk

*Corresponding authors

[1]Institute of Behavioural and Neural Sciences

[2]Centre of Biophotonics

[3]School of Psychology and Neuroscience, University of St Andrews, St Andrews, KY16 9JP, United Kingdom

Abstract

Stored product insect pests, like *Tribolium castaneum* beetles, cause 20% of postharvest loss. However, how their nervous systems coordinate adaptive movements for successful infestation is unknown. Here, we assess how *Tribolium* larvae locomote over different substrates and analyze their gait kinematics across speeds. Unlike many hexapods, larvae employ a bilaterally symmetric, posterior-to-anterior wave gait during fast locomotion. During slow locomotion, thoracic intrasegmental coordination is disrupted, whilst intersegmental coordination is preserved. Additionally, terminal abdominal structures (pygopods) support challenging locomotion, such as climbing overhangs. The onset of pygopod engagement coincides with leg swing initiation, suggesting a stabilizing role. Surgically severing the connective between thoracic and abdominal ganglia impaired pygopod engagement and impeded flat-surface locomotion, climbing, and tunnelling without interrupting leg kinematics. These results suggest that thoracic-abdominal coordination underlies effective movement, and gait/limb recruitment is context-dependent. Our work provides the first kinematic analysis of *Tribolium* larval locomotion and insights into its neural control.

Introduction

Stored product insects are devastating agricultural pests. These animals have been estimated to cause 9% of postharvest loss in developed countries and 20% in developing countries (reviewed in[1]). The red flour beetle, *Tribolium castaneum (Tribolium),* is representative of many stored product pest insects presenting a major challenge to global food security. Larvae and adults consume wheat products like flour by efficiently moving over and tunnelling through these unstable, shifting substrates[2]. Therefore, understanding how *Tribolium* adapt their movements to heterogeneous and challenging terrain could provide insights into conserved principles of motor control whilst aiding the development of new pest control approaches.

Animals use various strategies for adapting movement to the environments in which they live, continuously monitoring and adjusting movements on a cycle-by-cycle basis to cope with unexpected obstacles and/or drastic variations in the physical properties of 3-dimensional terrain. Studying the neural control of movement adaptability has

been a long-standing focus of motor systems research across multiple species. Terrestrial animals with internal, external, or hydrostatic skeletons have all evolved different strategies for movement control in different contexts (reviewed in insects[3,4], mammals[5] and birds[6]). Some animals deploy limbs[7–9], some utilize soft outer cuticular features[10,11] and others adapt body parts not typically involved in locomotion to solve motor problems[12]. Similarly, *Tribolium* exhibit a diverse behavioral repertoire in response to different sensorimotor cues, and adult anatomy has been well-described. Previous work has shown that *Tribolium* can move through a variety of stored grain, but prefer finely grained, whole wheat flour over coarser bran[13]. Moreover, adults can navigate in response to attractive and aversive odors[14,15], shapes[16], light levels[17], colors[18], and different habitat cues[19]. Both larvae and adults have articulated, jointed limbs[2], with larvae being composed of both soft ventral cuticle and semi-hardened dorsal cuticle. While anatomical studies have begun to characterize the larval neuromuscular system[20], knowledge concerning the specific kinematics of locomotion and how the *Tribolium* nervous system recruits thoracic limbs and abdominal segments to meet different locomotor demands is extremely limited.

Past studies have prioritized adult anatomy and behavior, although larval instars are equally capable of maneuvering and colonizing stored grain. Here we characterize locomotor parameters in late-instar *Tribolium* larvae to gain insights into how these animals adapt movements to their environment. We analyze how larvae negotiate different substrates and combine whole-animal and leg tracking to characterize and quantify leg kinematics underlying a range of locomotor speeds. We find larvae have an ethologically relevant preference for fibrous substrates and walk primarily with a posterior-to-anterior-propagating bilaterally symmetric gait, which shifts towards uncoordinated exploratory movements at slower speeds. Severing the connectives between thoracic and abdominal segments impairs walking, climbing, and tunneling but does not disrupt fundamental leg kinematics. In addition, we characterize a pygopod planting behavior, abolished in animals with severed connectives, which is used for stability and propulsion under different motor contexts (challenged locomotion vs tunnelling). These results provide first insights into the biomechanical underpinnings of *Tribolium* movement and the neural basis of ethologically relevant motor programs in an insect species with direct impacts on global food security.

Results

Tribolium castaneum life cycle, morphology, and substrate preference

Tribolium beetles take approximately 35 days at 29ºC to undergo complete metamorphosis, comprising four distinct developmental stages – egg, larval, pupal, and adult[21] (Fig. 1a). The larval stage is characterized by three thoracic segments, each supported by a pair of legs, and nine abdominal segments. Larvae possess two small, rounded ventral pygopods in the most posterior abdominal segment, and two spiked urogomphi dorsally (Fig. 1b).

We first established larval substrate preference based on ease of locomotion. We found larvae crawl best on textured, fibrous, wood-based substrates such as paper, cardboard, and lens paper (Fig. 1c). In contrast, they had substantial difficulty gripping smooth surfaces like plastic and glass, thus preventing forwards momentum. Similarly, their legs slipped on or stuck to deformable substrates like Sylgard™ and agarose, also impeding coordinated progress (Fig. 1d-e). Notably, on these substrates, we observed pygopod planting for substrate engagement in an anchoring motion, which, when released, propelled the larvae forwards (Supplementary Movie 1). This abdominal engagement was rarely observed on fibrous substrates. Surprisingly, crawling was heavily impeded over whole wheat flour and white flour (Fig. 1c-e), as larvae attempted to tunnel upon contact with these substrates.

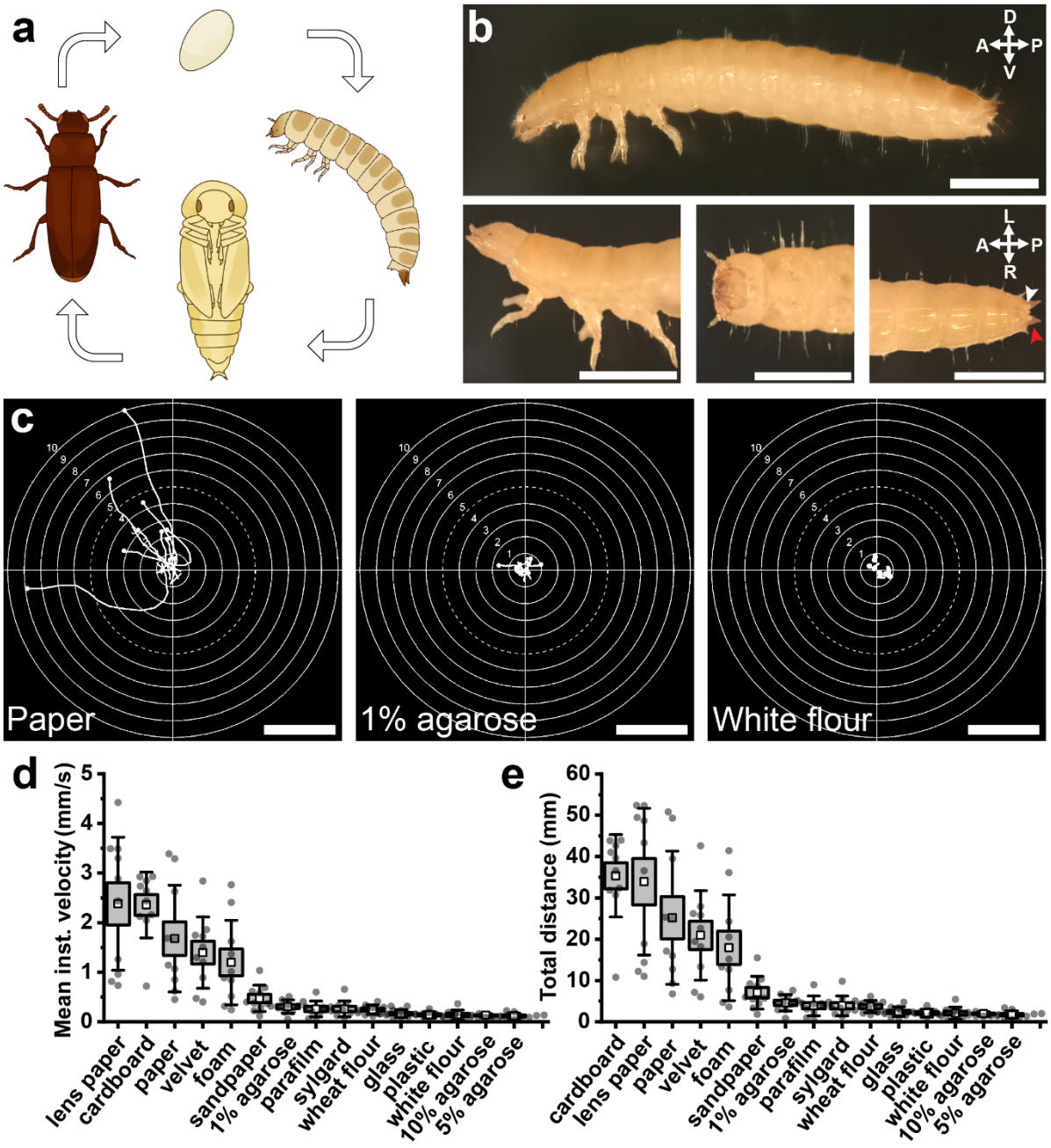

Figure 1: *Tribolium castaneum* life stages, larval morphology, and locomotor capability over different substrates. (a) Diagrammatic representation of *Tribolium castaneum* life cycle. **(b)** Morphology of 4th-5th instar larva under a 10x objective. Full body image at 2x magnification and insets at 5x magnification showing three thoracic leg pairs, nine abdominal segments, pygopods (white arrow) and urogomphi (red arrow). Scale bars = 1mm. **(c)** Larval paths over select substrates during first 15 seconds of free locomotion. Scale bar = 10mm. **(d)** Box plot of mean instantaneous velocity across fifteen substrates, ordered highest to lowest. **(e)** As **(d)**, for total distance travelled. White squares = mean, boxes = mean ±SE, whiskers = ±SD overlayed on raw data; n = 10.

103 **Quantifying larval locomotor parameters**

104 Next, movement parameters during free locomotion were analyzed to quantify the
105 spectrum of larval motor capabilities. Paper was used as the default substrate in
106 subsequent experiments given larval preference, accessibility, and ease of imaging.
107 *Tribolium* larvae exhibited heterogeneous walking patterns, and favored edge
108 exploration, i.e., they rarely strayed from arena edges once they found them (Fig. 2a).
109 Additionally, we observed persistent burrowing attempts at the paper edges during
110 preliminary trials in which the paper substrate was not fully adhered to the arena
111 platform.

112 Locomotion on paper had a mean instantaneous velocity of 1.8 ± 0.1 mm/s (range =
113 0.9 to 3.0 mm/s; larval sizes ranged 4-6 mm), and animals displayed a spectrum of
114 intra-animal velocity variability during only 2 minutes of exploration (Fig. 2b). Faster
115 animals were not constantly fast, but instead varied speed throughout locomotion,
116 whereas slower animals were limited to lower speed ranges (Fig. 2c). Larvae spent
117 equal time walking straight (49.6%) and turning (50.4%) (Fig. 2d). Animals decelerated
118 to turn but rarely stopped completely, thus staying immobile only 0.5% of the time (Fig.
119 2d). Finally, most larvae did not show a bias in turning direction, engaging equally in
120 left and right headsweeps during exploration (Fig. 2e).

121 We observed a larval motor program we termed "backtrack and redirect"
122 (Supplementary Movie 2), defined as a headsweep/turn in one direction, followed by
123 visible backwards locomotion, and a contralateral headsweep/turn and forwards
124 locomotion (Fig. 2f), which on average lasted 3-6 seconds. This behavior followed a
125 distinct sequence of instantaneous velocity and body angle changes. First, velocity
126 dropped as the animal turned (body angle deviating from 180º), followed by an
127 increase in velocity at 180º body angle due to backtracking, and ended with another
128 deceleration and deviation from 180º in the opposite direction from the animal's
129 original trajectory (Fig. 2g). While 63.3% of larvae displayed this motor program at
130 least once during 2 minutes of free locomotion (Fig. 2h), some displayed it a maximum
131 of 8 times, and a third never engaged in this behavior.

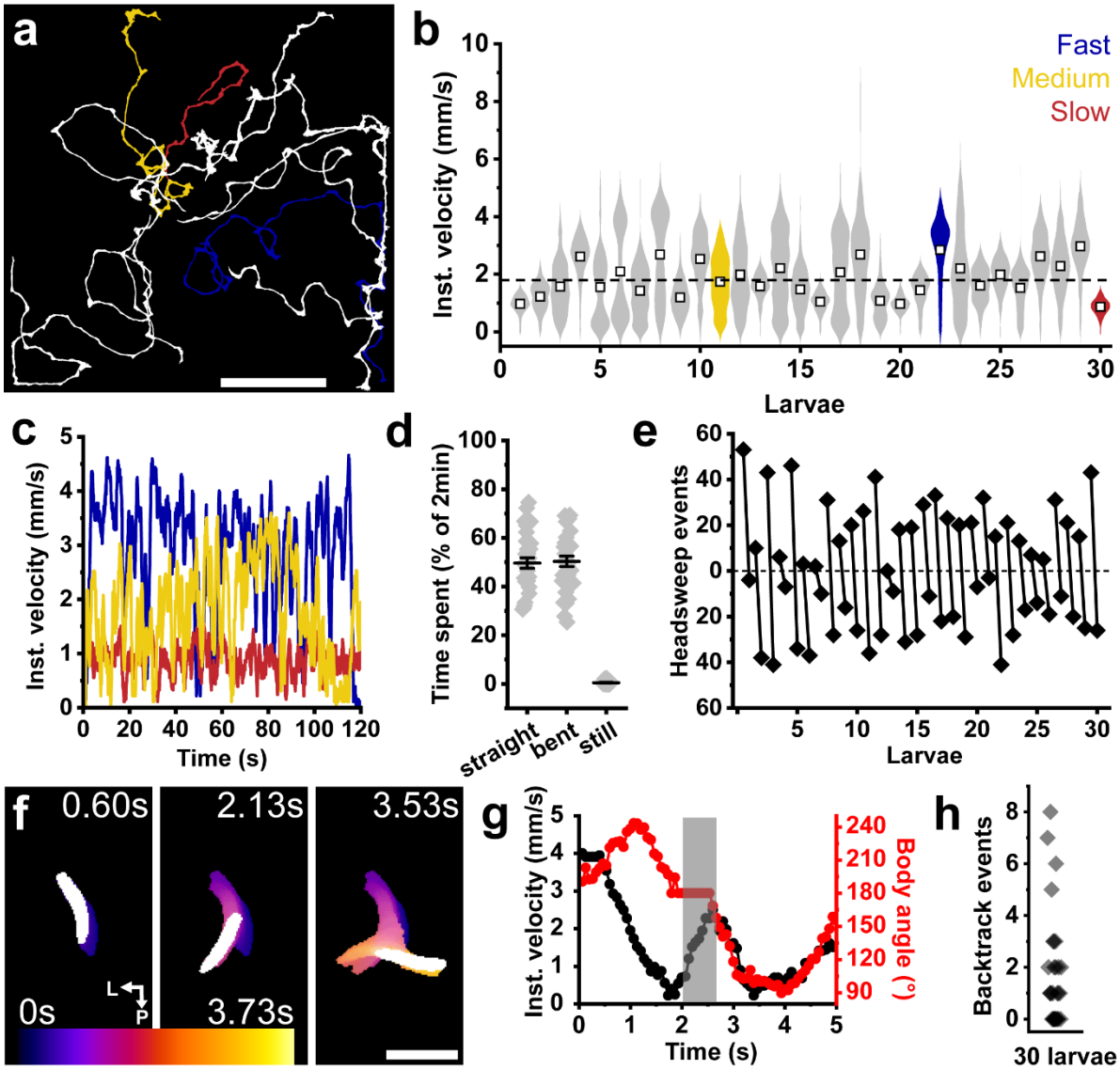

Figure 2: Inter- and intra-animal variability in free locomotion parameters. (a) Select larvae's paths of free locomotion across white paper for 2 minutes. Colored paths represent fast (blue), intermediate (yellow) and slow (red) larvae based on mean instantaneous velocity. Scale bar = 5cm. **(b)** Violin plot showing intra-animal variability in instantaneous velocity. White squares = mean. **(c)** Instantaneous velocity traces across 2 minutes of colored animals in **(a)** highlighting inter- and intra-animal variability. **(d)** Proportion of time spent in distinct locomotor behaviors: straight = 180° body angle and >0mm/s velocity, bent = non-180° body angle and >0mm/s velocity, still = 0mm/s velocity regardless of body angle. Whiskers = mean ±SE, n = 30. **(e)** Total headsweep events by individual larvae. Left headsweep = ≥210° body angle, right headsweep = ≤150° body angle. **(f)** 3 frame sequence during a backtrack and redirect behavior. Frames are color-coded for total time (3.73s); temporal larval trajectory is overlayed beneath current frame (white). Note the center frame showing more posterior body position relative to preceding frames, indicative of "backtracking". Scale bar = 5mm. **(g)** Instantaneous

velocity and bodybending angle against time during backtrack and redirect behavior sequence. Gray area highlighting backwards locomotion. **(h)** Total number of backtrack and redirect events during two minutes of free locomotion, n = 30.

Gait coordination and leg kinematics across walking speeds

To characterize natural gait, leg kinematics and the coordination between thoracic segments, we tracked legs during straight walking bouts on paper. We found *Tribolium* larvae walked with a bilaterally symmetric posterior-to-anterior wave gait (Fig. 3a). Then, we determined the frequency of locomotion for each animal by performing a Fourier transform on leg velocities and selecting the frequency with highest power of an anchor leg (left T1). We defined swing phases by a leg's lifting and planting on the substrate and stance phases as the duration in which legs are in contact with the ground. An average cycle period was then calculated for each leg. After a swing, legs usually stanced next to the legs of the segment in front, and these often began their swing phase before the previous contacted the ground (Fig. 3a). This pattern was observed most prominently within the T2 to T1 transition as their swing phases overlapped more visibly (Fig. 3b-d).

Fast (Fig. 3b, d, f) and slow (Fig. 3c, e, g) walk cycles differed markedly. In faster animals, typical walk cycles averaged 0.2 ± 0.007s and were initiated by a T3 swing phase, followed by T2 with a phase delay of approximately 120º, then T1 with another 120º delay. These delays were largely consistent between legs and across animals, independent of speed (Fig. 3h). In fast animals, many legs were significantly coherent with each other (Fig. 3j). In slower animals, average cycle period was 0.7 ± 0.1s, and some legs often swung alone during walk cycles (Fig. 3e). Furthermore, not all six legs were required to swing during each cycle. Absent leg swings consequently impaired intrasegmental coordination; phase differences between contralateral leg pairs increased (binned mean for 5 slowest larvae = 41.0 ± 7.5º) compared to faster animals (binned mean for 5 fastest larvae = 15.1 ± 3.4º) (Fig. 3i). As such, fewer legs were significantly coherent to each other in slower animals (Fig. 3j), but the T3 to T1 sequence was largely preserved (Fig. 3h). Finally, analysis of all swing and stance phases against cycle period showed stance duration increased with cycle period, whilst swing duration was constant (Fig. 3k). Therefore, swing and stance duty cycles,

defined as the proportion of time normalized to the cycle period, showed opposing exponential relationships with cycle period (Fig. 3l).

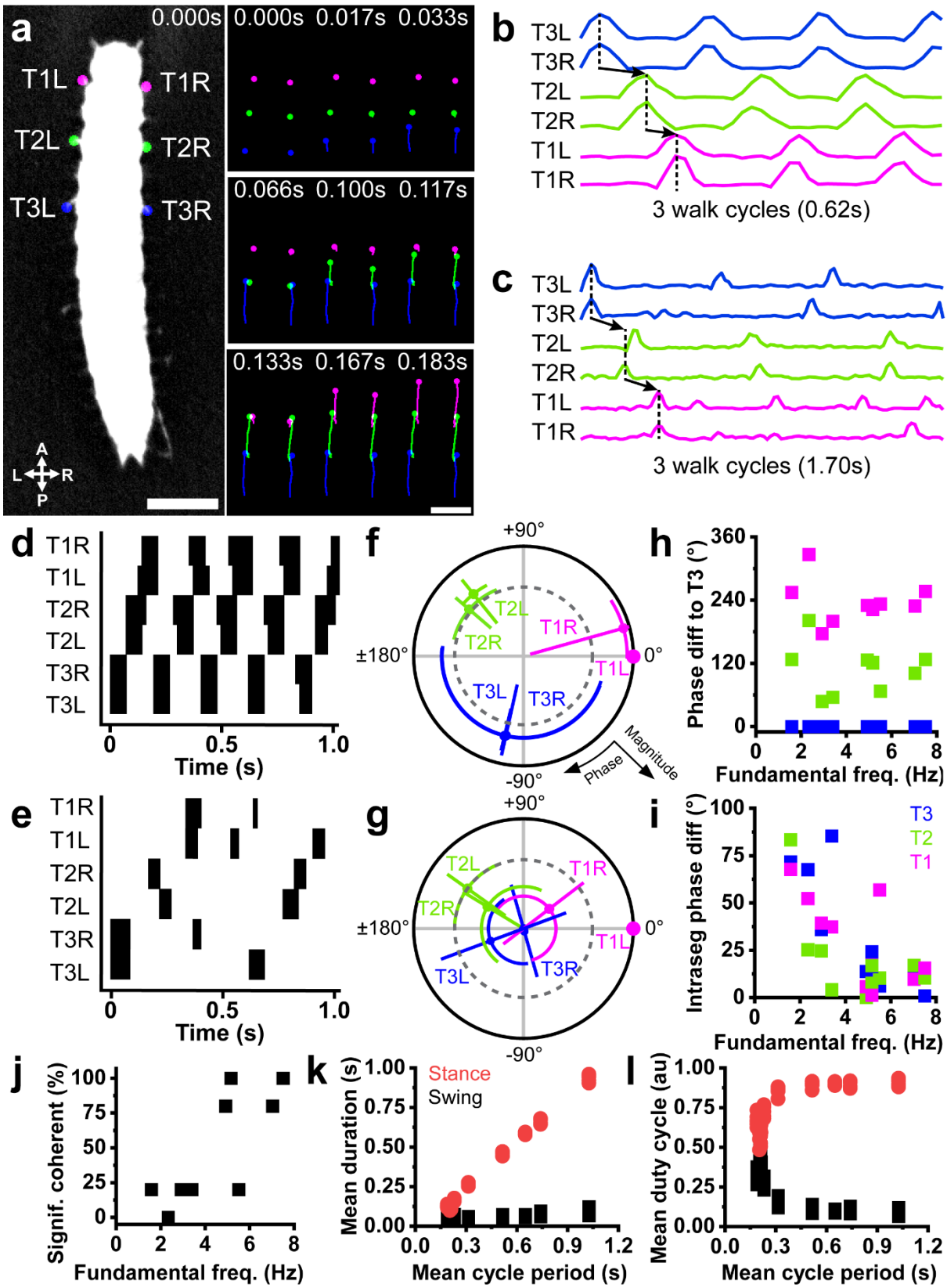

178 **Figure 3: Gait coordination and leg kinematic coherence are largely speed dependent.**
179 **(a)** Left: example top-down view of *Tribolium* larva with labelled legs across three thoracic
180 segments: T3 (blue), T2 (green) and T1 (magenta). Scale bar = 1mm. Right: select frames of
181 tracked leg positions showing progression from T3 to T1 in one representative walk cycle.
182 Note the bilateral symmetry as leg pairs swing. Scale bar = 1mm. **(b-c)** Example velocity traces
183 of legs for **(b)** fast and **(c)** slow animals across three walk cycles. Note the greater
184 intersegmental coordination in **(b)** than **(c)**. **(d-e)** Swing (black) and stance (white) phases in
185 the same **(d)** fast and **(e)** slow animals in **(b-c)**. **(f-g)** Polar plots of coherence phase and
186 magnitude of waveforms in **(b-c)** using T1L as anchor/0° for **(f)** fast and **(g)** slow animals.
187 Negative phase values temporally precede positive ones. Dark grey dotted inner circle
188 indicates α = 0.05 for coherence magnitude. **(h)** Scatter of phase difference between left legs
189 of each segment and T3 across fundamental frequencies (proxy for walking speed). **(i)** Scatter
190 of phase difference between legs of each segment. **(j)** Percentage of significantly coherent
191 legs (out of 5) to anchor (T1L). **(k)** Mean swing and stance durations and **(l)** duty cycles for
192 individual legs as a function of cycle period averaged across 3-5 tracked cycles per leg. N =
193 10.

194 **Effects of severing thoracic-abdominal connectives on locomotion and climbing**

195 To begin to understand the neural control of movement in *Tribolium* larvae, we severed
196 the connective between thoracic and abdominal ganglia (Fig. 4a-b) to assess the
197 effects of interrupting ascending and descending connections between brain and
198 suboesophageal ganglion (SOG) and ventral nerve cord (VNC) on unrestrained
199 locomotion. Severed animals travelled significantly less far (mean = 5.83 ± 0.58cm)
200 on paper than controls (mean = 13.3 ± 2.0cm, p = 0.020) and sham treated animals
201 (mean = 14.4 ± 2.0cm, p = 0.008; Fig. 4c-d). Moreover, they displayed a narrower
202 range of body bending angles (range = 115.8 to 224.1º) than controls (range = 122.7
203 to 245.4º) and shams (range = 111.0 to 273.2º) (Fig. 4e). To see how these
204 impairments affected performance during a locomotor challenge, we first performed
205 preliminary experiments gauging control larvae performance on different inclinations
206 (Supplementary Figure 1): 180º (flat surface), 135º (uphill), 90º (vertical wall), and 45º
207 (overhang). We found control animals walked progressively less far with greater
208 deviations from 180º but were still able to cling onto and climb 45º overhangs.
209 Interestingly, larval paths became straighter, and fewer animals approached arena
210 edges with greater inclination.

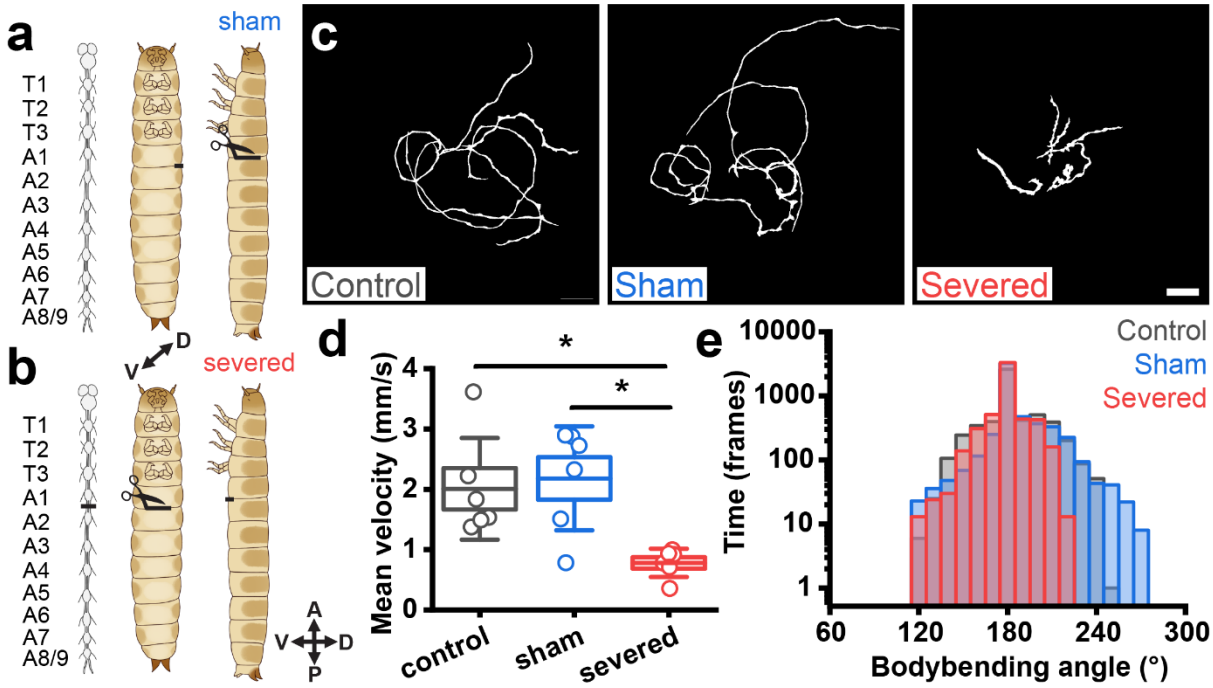

211 **Figure 4: Severing thoracic-abdominal connectives impairs locomotion and restricts**
212 **bending. (a-b)** Surgical manipulations for **(a)** sham: lateral lesion between A1-A2 and **(b)**
213 severed: ventral severing of the A1-A2 connectives. **(c)** Walk paths on paper across
214 treatments for 1 minute. Scale bar = 2cm. **(d)** Box plots of mean instantaneous velocity. Boxes
215 = mean ±SE, whiskers = ±SD; * p<.05, One-way ANOVA, n = 6. **(e)** Frequency plot of all body
216 angles throughout 1 minute of locomotion, binned every 10º. Note the exponential y axis
217 (log10).

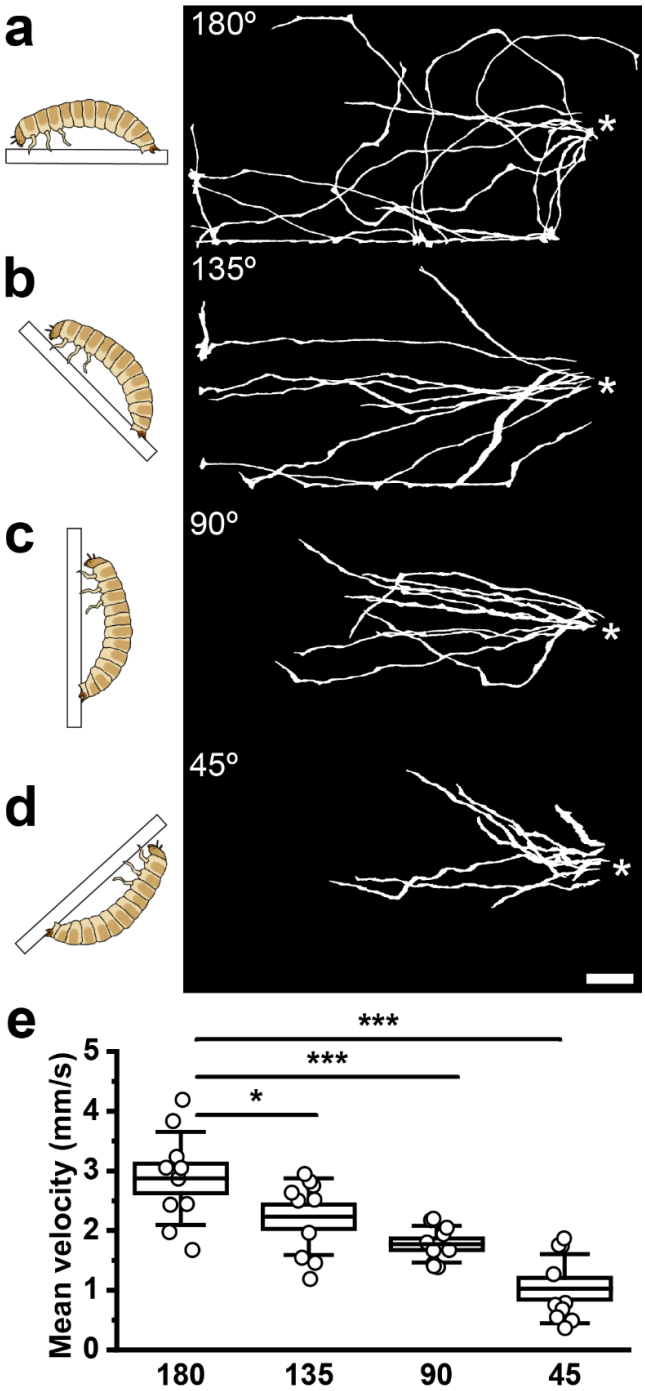

Supplementary Figure 1: Increasing incline becomes progressive locomotor challenge for *Tribolium* larvae. (a-d) To the left, diagrams of larval orientations relative to angled platforms and to the right, walk paths of larvae at varying inclines. Note 45º is an overhang. Asterisks indicate starting position. **(e)** Box plot of mean instantaneous velocity across inclinations. Boxes = mean ±SE, whiskers = SD; *** p<.001, * p<.05, One-way ANOVA, n = 10.

224 Next, we used inclines as a motor challenge for severed animals to investigate how
225 disconnecting the abdominal nervous system would affect clinging and climbing during
226 challenged locomotion. Control, sham, and severed animals were tested on 180º, 135º
227 and 45º. Severed animals exhibited prominent clinging and climbing impairments –
228 42.9% at 135º and 71.4% at 45º of larvae failed to cling on and fell (represented as
229 0mm/s points for velocity in Fig. 5b). Severed animals that could cling and climb had
230 straightening paths and slower speeds with increasing incline, as was observed in
231 control and sham treated animals (Fig. 5a-h). As expected, severed speeds were
232 significantly lower for baseline 180º (control-severed, $p<.001$; sham-severed, $p=.002$)
233 and 135º (control-severed, $p<.001$; sham-severed, $p=.007$). Nonsignificant differences
234 at 45º may reflect an overall speed limitation at such extreme inclinations.

235 To assess leg kinematics and coordination differences across treatments and
236 inclinations, we observed locomotor performance on 180º and 45º inclines on an up-
237 close incline behavioral rig as opposed to the top-down view (Supplementary Movie
238 3, Supplementary Movie 4). At 45º, 14.3% of severed animals fell, and 42.9% clung
239 on but remained immobile. Consequently, these animals were excluded from
240 locomotor and kinematic analysis. Notably, no control or sham animals fell at any
241 inclination in either experiment. To effectively compare locomotion across conditions,
242 walk cycles following the T3 to T1 gait sequence were analyzed. Severed animals
243 were slower overall but followed locomotor parameter trends in control and sham for
244 180º. However, they were indistinguishable from controls and shams at 45º as overall
245 locomotion slowed. Swing/stance durations and duty cycles followed the same trends
246 with speed observed previously (Fig. 3k-l) independent of inclination; stance duration
247 was modulated, whilst swing duration remained constant across speeds (Fig. 5i-j, m-
248 n). Stride lengths increased linearly with speed at both 180º ($r^2 = .754$, $p<.001$; Fig.
249 5k) and 45º ($r^2 = .387$, $p<.001$; Fig. 5o), and intersegmental differences were
250 proportional across treatments and inclinations (Fig. 5l, p).

251 At 45º, only control and sham larvae engaged their pygopods to assist climbing
252 (Supplementary Movie 4), which suggested climbing required descending inputs to the
253 abdomen. Moreover, larvae consistently attempted to maintain abdominal contact with
254 the substrate, suggesting sustained contraction of body wall muscles whilst climbing.
255 Pygopod planting events were defined as visible pygopod extensions, and a change

from a parallel alignment with the substrate to a perpendicular pointed orientation into it (Fig. 5q). Analysis of their relation to leg kinematics in all walk cycles showed that most pygopod planting events coincided temporally with the initiation of leg swing phases (Fig. 5r), and pygopod planting-triggered analysis showed the sequence from T3 (blue) to T1 (magenta) as seen by the peaks in the distributions (Fig. 5r). Moreover, pygopod engagement was preceded by an increase in velocity and followed by a decrease (Fig. 5s), consistent with the association between pygopod planting events and leg swings. Although most control and sham larvae engaged their pygopods on the overhang (mean rate = 0.76Hz, range = 0 to 1.20Hz), this did not significantly correlate with their maximum velocity (r^2 = .123, p = .092) (Fig. 5t).

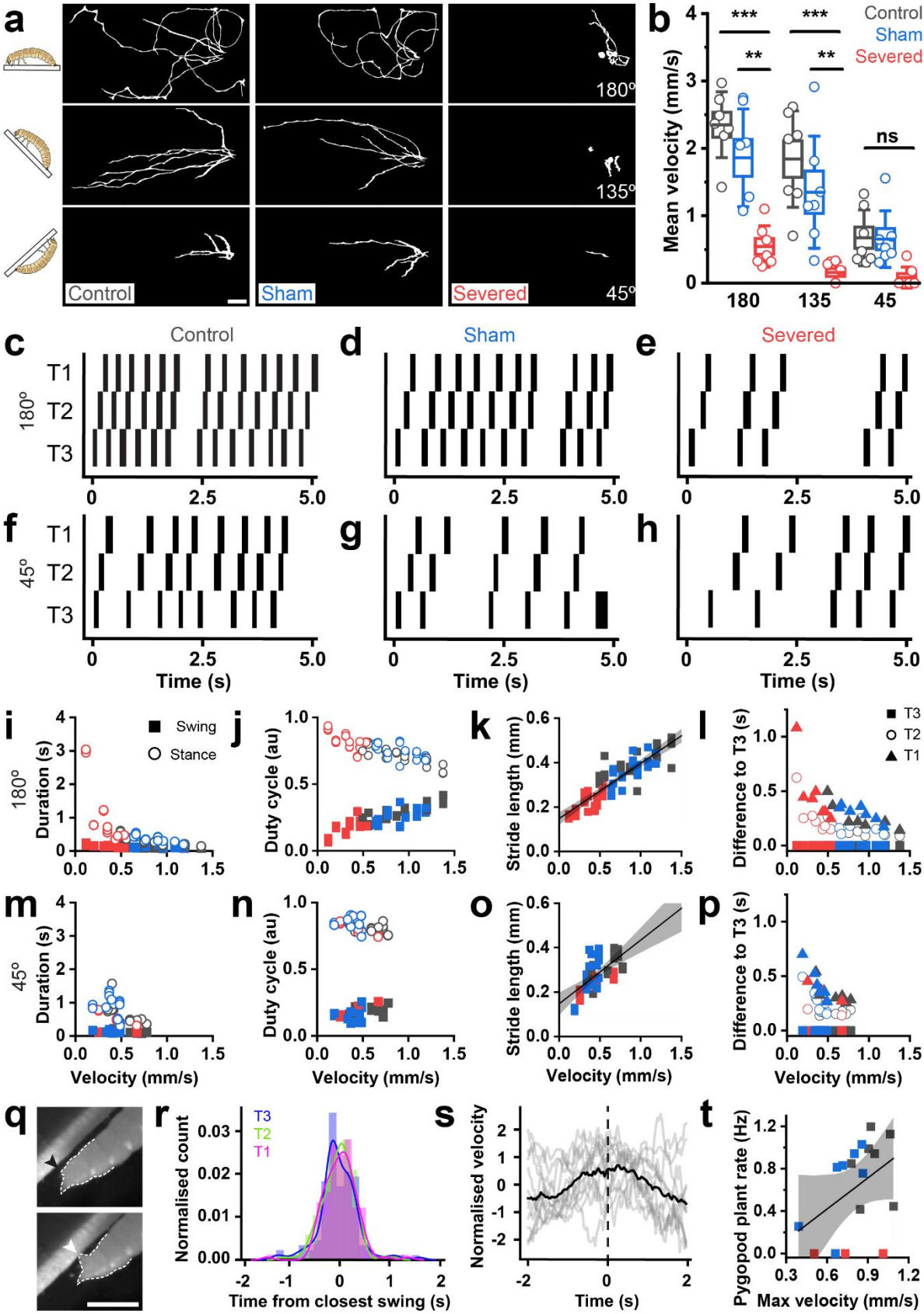

266 **Figure 5: Abdominal inputs are not required for thoracic coordination and pygopods**

provide stability in locomotion. (a) Walk paths of control, sham, and severed larvae on top-down incline rig. Scale bar = 2cm. **(b)** Box plots of mean instantaneous velocity of tracked larvae. Boxes = mean ±SE, whiskers = ±SD; *** p<.001, ** p<.01, One-way ANOVA, n = 7. **(c-h)** Representative swing (black) and stance (white) phase plots of walk cycles following T3 to T1 sequence on up-close incline rig. Note the prolonged stance phases in severed at baseline 180º. **(i-p)** Scatter plots comparing locomotor parameters: **(i, m)** swing/stance duration, **(j, n)** swing/stance duty cycle, **(k, o)** stride length and **(l, p)** time difference to T3 (intersegmental difference). All values are averaged per leg; velocity is mean across walk cycles. **(k, o)** Stride length correlates significantly with velocity at 180º (r^2 = .754, p < .001), and 45º (r^2 = .387, p < .001). **(q)** Frames showing pygopod relaxation parallel to substrate (black arrow) and planting into substrate (white arrow). Scale bar = 1mm. **(r)** Histogram of normalized pygopod planting event count relative to initiation of closest leg swing across all walk cycles, binned according to the Freedman–Diaconis rule (see Methods). Note the order of distribution peaks highlights predominant T3 to T1 gait even in unfiltered walk cycles. Total number of leg movements = 117 per leg. **(s)** Normalized mean instantaneous velocity (black trace) relative to pygopod planting events (dotted line); individual velocities across 13 larvae (control and sham combined) in grey. **(t)** Pygopod plant rate correlates insignificantly and weakly with maximum velocity (r^2 = .123, p = .092). N = 7 per treatment.

Abdominal contributions in tunnelling

As evidenced, abdominal inputs (ascending or descending) facilitated free locomotion on flat surfaces and during locomotor challenges. Although clinging and climbing behavior may assist *Tribolium* in navigating and infesting food storage systems, we wanted to probe the effects of severing thoracic-abdominal connectives on tunnelling into their food source. Larvae (control, sham and severed) were individually dropped onto a dish filled with approximately 6mm deep whole wheat flour and visible body length was measured 0s and 120s afterwards (Fig. 6a-f). Control and sham animals immediately tunneled into flour on contact, as observed previously during substrate preference tests, with 100% of control and 75% of sham larvae being fully submerged after 2 minutes (Fig. 6g). Strikingly, 0% of severed animals tunneled effectively into flour, and on average, 90.7% of their original body lengths was exposed after 2 minutes

297 (Fig. 6h). Severed animals still visibly displaced flour with their legs, albeit without
298 making any progress (Fig. 6f). Therefore, the abdominal segments are essential for
299 larval submergence into flour.

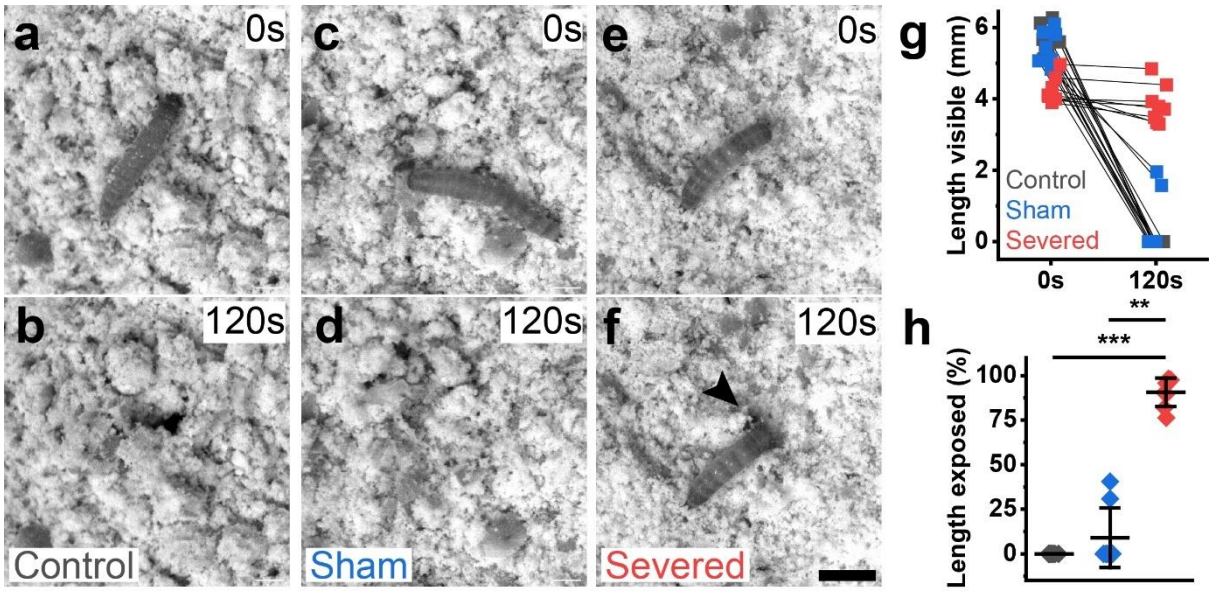

300 **Figure 6: Abdominal inputs are crucial for larval tunnelling into natural food source. (a-**
301 **f)** Top-down frames at 0s and 120s after placement on flour for **(a-b)** control, **(c-d)** sham and
302 **(e-f)** severed animals. Severed animals struggle to tunnel; black arrow indicates displacement
303 of flour from thoracic leg movements despite no body submergence. Scale bar = 2mm. **(g)**
304 Change in body length between 0s and 120s across treatments. **(h)** Percentage of original
305 body length exposed after 120s. Whiskers = mean ±SE; *** p<.001, ** p<.01, Kruskal-Wallis
306 test, n = 8.

307 ## Discussion

308 To study and understand the *Tribolium* larval abdomen's roles in locomotion and its
309 relationship to the legs, we first characterized the larva's general locomotor
310 performance across a range of conditions. We found larvae relied on their legs for
311 unchallenging locomotion on preferred substrates, which mostly consisted of fibrous
312 materials. This supports the hypothesis that their original habitat consisted of tree
313 bark[2,22], and explains why wet, slippery surfaces present a challenge. While adults are
314 capable of locomotion across flour[23], tunnelling is the primary motor program for
315 navigating their food source during pre-pupal instars**.** This behavior reflects
316 ethologically relevant photophobic preferences[17] and their propensity to tunnel deeper

317 when approaching pupation[24]. The locomotor patterns underlying their exploratory
318 behavior consist of straight runs and continuous turning, with little to no periods of
319 immobility. This differs from *Drosophila* larvae, which combine repeated straight runs
320 with pauses followed by headsweeps, redirecting them to a new trajectory[25,26].
321 *Tribolium* larvae also show no evidence of handedness in their exploratory
322 movements, again in contrast with *Drosophila* adults[27] and larvae[28] but also other
323 insects such as ants[29] and cockroaches[30]. This may reflect the requirements for
324 *Tribolium* to navigate a 3-dimensional environment of constantly shifting substrate. We
325 also found a larval preference for edge exploration, which may represent
326 photophobicity, centrophobicity or a thigmotactic drive to maximize body contact with
327 their environment to mimic how they are naturally enveloped in substrate. This
328 behavior is also found in *Drosophila* adults, but not for centrophobic or thigmotactic
329 reasons[31].

330 The most common gait in insects is the alternating tripod gait, in which the first and
331 third leg on one side of the body move together with the contralateral second leg[32].
332 *Tribolium* larvae, however, use a travelling wave gait, involving posterior-to-anterior
333 sequences of swings propagating from T3 to T1 across all walking speeds. Their
334 contralateral leg pairs move synchronously, and phase delays between segments are
335 largely maintained across speeds. This bilaterally symmetric travelling wave gait is
336 found in the larvae of other beetles, including leaf beetles[33,34]. Since environmental
337 conditions do not differ between larval and adult stages in these animals, the wave
338 gait could therefore reflect developmental constraints on the circuit architecture driving
339 locomotion in the Cucujiformia infraorder of beetles. However, the travelling wave gait
340 pattern is found more widely. For example, in krill and crayfish, it generates the forces
341 required for locomotion in an aquatic medium[35,36], and in some millipedes it is used to
342 generate the required forces for burrowing in soil[37]. A similar bilaterally symmetrical
343 gait has been observed in the dung beetle *Pachysoma endroedyi*. In their 'galloping'
344 gait, the anterior two leg pairs move in a travelling wave, with the hind leg pair dragging
345 behind them and contributing little to forwards motion[38]. In these desert dwelling
346 species, in-phase contralateral coordination may be energetically favorable for
347 traversing constantly shifting terrains like sand, a constraint they might share with
348 aquatic species. These considerations are equally relevant for *Tribolium,* as they
349 consume and inhabit a constantly deformable substrate. This gait may become

350 particularly beneficial during *Tribolium* pre-pupal stages, when larvae tunnel deeper
351 for warmth and lower population densities to prepare for pupation[24].

352 Many animals display speed-dependent gait transitions. For example, adult
353 *Drosophila* gaits have been shown to transition from a pentapodal wave (one leg is in
354 swing phase at a time) to a tetrapodal (two legs, but not bilateral pairs) and finally
355 tripodal wave (three legs) by modulating stance phases as the animal progresses from
356 slow to fast speeds[39]. Gait adjustments tune movement to the requirements of different
357 terrains and speeds of locomotion[38,40–44]. We therefore also characterized the
358 kinematic changes accompanying different speeds of locomotion in *Tribolium* larvae.
359 They similarly have increasing numbers of limbs in swing phase at a time during
360 increasingly fast locomotion, but do not appear to adopt a gait other than their
361 bilaterally symmetrical metachronal wave. Moreover, larval stride length increases
362 linearly with speed, following a highly conserved locomotor strategy across
363 invertebrates and vertebrates[45–47]. A similar in-depth analysis of adult *Tribolium* gait
364 kinematics in the future will allow further comparison.

365 The *Tribolium* VNC is unfused, with a separate ganglion in each body segment,
366 chained together by longitudinal connectives, and each thoracic ganglion innervating
367 a leg pair[48,49]. This anatomical arrangement is found across arthropods[50] and
368 tardigrades[51], and suggests gait variation across and within species might be derived
369 from one single modifiable control strategy[52]. This raises the question whether the
370 neural control of its behavior shares similarities with that of the more well-studied and
371 soft-bodied *Drosophila* larva, which is legless and moves by means of abdominal
372 peristaltic waves[26], and has a segmentally fused central nervous system[53].

373 Qualitatively observed pygopod planting during unrestricted motor programs
374 (backtrack and redirect, see Fig. 2f) first suggested a prominent role for the abdomen
375 in assisting natural movement. We present several lines of evidence that pygopods
376 act to support locomotion in challenging conditions. First, while fast animals crawling
377 on level fibrous surfaces do not necessitate pygopod engagement, they do while
378 climbing 45º overhangs. Furthermore, pygopod planting events are largely temporally
379 locked to leg swing phases, during which the animal needs to maintain static stability,
380 and these events are preceded by a temporary increase in crawling speed. This shows
381 a correlation between situations that compromise the animal's stability and likelihood

382 of pygopod engagement. Furthermore, the weak, non-significant correlation between
383 pygopod planting rate and maximum velocity further implicates its role in stability over
384 a mechanism to boost/propel overall speed. Second, severing the A1-A2 connective,
385 thus removing descending and ascending inputs between the brain, thorax and
386 abdominal segments, resulted in lower speeds during walking and climbing. Some
387 severed animals dragged their abdomen during walking (Supplementary Movie 3),
388 which may contribute to decreasing velocity as the lack of abdominal sensory inputs
389 may impair its ability to support itself during locomotion. However, impairments on
390 inclines varied, ranging from some severed animals falling off mild (135º) inclines to a
391 select few matching control and sham performance on 45º overhangs. The latter may
392 reflect the overhang limiting the feasible speeds larvae can produce in this motor
393 challenge. Like the variability in inter-animal velocities in normal larvae, the severity of
394 severing is likely equally dependent on the individual. Nevertheless, severed animals
395 never engaged their pygopods, and most tended to fall off 45º overhangs. These
396 animals' inability to engage their posterior segments therefore particularly impaired
397 their locomotor capabilities under challenging conditions. Furthermore, this phenotype
398 is unlikely due to a failure to coordinate leg movements, since severed animals fall into
399 the same speed-dependent distributions of kinematic patterns including swing and
400 stance duration, duty cycle, stride length and intrasegmental phase difference as
401 control and sham larvae. This suggests that abdominal regions are not required for
402 fundamental leg coordination but provide a crucial support role in larvae.

403 Other species that have abdominal anchoring points with potential stabilizing roles
404 include *Labidomera clivicollis* larvae, which use pygopods during body extension
405 whilst climbing tree branches[33]; and blackfly larvae, which are adapted to anchor into
406 riverbeds to avoid getting swept away by strong currents[54]. The *Tribolium* larval
407 anatomical adaptations we describe that confer stability and allow the animal to stay
408 upright may similarly help evade predation, for example by the parasitoid wasp
409 *Holepyris sylvanidis*[55], either by enhancing locomotion efficiency in shifting terrain or
410 avoiding falling off tree branches in their original habitat. The use of posterior terminal
411 organs for substrate engagement during locomotion is also found in other soft-bodied
412 animals including *Drosophila* larvae[11], *Gastrophysa viridula*, which deploy their
413 pygopods phase-locked to leg movements during the locomotor cycle[56]; and *Manduca*
414 *sexta*, whose locomotor cycle starts with the terminal prolegs lifting off the substrate[4].

415 Our results elucidate a functional role for the pygopods, which were previously only
416 phenotypically mentioned in the *iBeetle* RNA interference (RNAi) screens[57,58].

417 The contribution of abdominal segments is likely to extend beyond offering physical
418 support during locomotion. During motor challenges like overhangs, larvae may send
419 ascending information from abdominal sensory neurons (e.g., regarding reduced body
420 contact with substrate) to sensorimotor integration centers for sensory feedback.
421 These may then integrate and send back descending information regarding internal
422 representations (e.g., current geotactic location, motor state) to make a higher order
423 decision to plant the pygopods to increase stability. Interruption of communications to
424 and from the abdomen and thus lack of stability in severed animals may explain those
425 that fall off or fail to climb. However, the severed animals that could cling and climb
426 followed the same leg kinematics as controls and shams, therefore lack of abdominal
427 input appears to not disrupt thoracic movements.

428 Furthermore, our data suggest the posterior segments have prominent functions in
429 tunnelling alongside stability. Tunnelling is a key motor program for navigation,
430 feeding, development, and reproduction in their natural habitat, and the inability to
431 tunnel in severed larvae suggests a crucial role for abdominal contractions, pygopod
432 recruitment, and/or ascending sensory feedback in coordinating effective tunnelling.
433 The abdomen may be recruited to generate pushing forces to submerge larvae in flour,
434 similar to millipedes[37]. Equally, it may aid exploratory movements such as the
435 backtrack and redirect behavior (Fig. 2f) to search for new food sources. Investigating
436 the structure of both ascending and descending inputs passing through the larval
437 *Tribolium* A1-A2 connective is therefore a promising avenue to explore the neural
438 basis of its behavior and could be a possible pinch point to disrupt the animal's ability
439 to infest grain stores.

440 Finally, *Tribolium* is an attractive emerging model system in behavioral neuroscience,
441 combining a robust experimental toolkit with an extensive body of work describing its
442 development and physiology. As the first coleopteran species to have a fully
443 sequenced genome (~16,500 genes), 47% of which are orthologous to insects and
444 vertebrates, *Tribolium* are already highly favored in the field of developmental
445 genetics[59]. Their genetic toolkit includes the GAL4-UAS system[60], CRISPR/Cas9
446 genome editing[61,62], balancer chromosomes, and stable injectable RNAi gene

silencing[63]. Forward genetic screens uncovered previously unknown genetic regulators of leg and body wall muscle development[20], and recent studies have described the structure and function of the *Tribolium* cryptonephridial system, which is essential for the animal's exceptional tolerance to desiccation[64]. The structures and locations of brain regions in larval and adult *Tribolium* showed broad similarities to other insect model organisms[65–67]. In addition, comparison of *Tribolium* and *Drosophila* larval neuromuscular systems revealed resemblances in somatic muscle composition[20]. Its similarities to both ancestral and highly derived insects therefore make it an attractive comparative model.

Overall, this study has emphasized how the kinematic analysis of movement and underlying neural control provides insights into natural behaviors that govern *Tribolium*'s success as a pest. We identified the importance of abdominal segments and pygopods to both locomotor challenges and tunnelling, suggesting that studying the structure and function of its connectives has important potential implications for behavioral neuroscience and food security. How far our findings extend to earlier instars and adults remains a promising question for future study.

Methods

Animals

Wild-type *Tribolium castaneum* (San Bernardino strain) were reared in 500ml borosilicate bottles with perforated lids (VWR SCOT291182809) at 29°C in organic wholewheat flour and 5% dried active yeast per weight. 4-5th instar larvae approximating 4-6mm in length were used in all experiments.

Statistics

Main text results and box plots are given as mean ±SE, and box whiskers are ±SD unless otherwise stated. Details of statistical analysis are included under each experiment's subsection below.

Substrate testing

Basic locomotor ability was tested on twelve substrates – white printer paper, cardboard, parafilm, lens paper, Sylgard™, glass, velvet, sandpaper, plastic, packing

476 foam, white flour, whole wheat flour, 1%, 5% and 10% agarose. Ten larvae were placed
477 in the center of the substrate and recorded for 1 minute. Movies were recorded with a
478 mobile camera (SM-A415F/DSN, Samsung, Seoul, South Korea) at 30fps and
479 analyzed with Fiji (Fiji is Just ImageJ)[68]. Larval head position was manually tracked for
480 the first 15 seconds (since larvae on preferred substrates often walked out of frame
481 within this time window) with the Manual Tracking plugin
482 (https://imagej.net/ij/plugins/track/track.html) for Fiji.

483 *Free locomotion assay*

484 30 larvae were placed in groups of 3-4 in a 18x18cm arena lined with white printer
485 paper and recorded for 2 minutes in darkness with a custom-built imaging setup using
486 an MQ013MG-E2 XIMEA CMOS (Ximea GmbH, Münster, Germany) camera with a
487 35mm C-mount lens (Thorlabs Inc, NJ, USA). Animals were illuminated with 850nm
488 infrared light using a Thorlabs M850L3 LED (Thorlabs Inc, NJ, USA). Larvae were
489 tracked with FIMTrack[69].

490 *Gait characterization*

491 Ten larvae were placed on white printer paper under an Olympus SZX10 (Olympus
492 Microscopes, Tokyo, Japan) dissection microscope at 0.8x magnification using a 0.5x
493 objective. Animals were recorded with an MQ042RG-CM XIMEA CMOS (Ximea
494 GmbH, Münster, Germany) camera at 60fps. 3-5 straight walk cycles were extracted
495 and manually tracked with Fiji's Manual Tracking plugin. Gait dynamics and locomotor
496 parameters were analyzed with Python scripts for individual legs; cycle period was
497 calculated as 1 over average cycle frequency. A Savitzky-Golay low-pass filter was
498 applied to manually tracked velocities to discretize swing durations. Stance duration
499 was calculated as the period between consecutive swings. Duty cycle was calculated
500 as average swing/stance duration over average cycle period. Intrasegmental phase
501 difference represents the phase difference between left and right legs within each
502 thoracic segment. Intersegmental phase difference represents phase difference of left
503 legs in each segment relative to left T3.

504 Coherence and phase analysis was performed with MATLAB application *Groundswell*
505 (https://github.com/JaneliaSciComp/Groundswell). A fast Fourier transform was
506 performed on the anchor leg's velocity trace to determine its spectral composition. The

507 anchor's fundamental frequency was determined as the frequency with greatest power
508 density (i.e., during swing phases) in the power spectrum. If the highest power
509 frequency was ambiguous (i.e., appeared as blocks of plateaus on the spectrum), the
510 middle value within the plateau was chosen, and the higher frequency block was used
511 in cases with two adjacent blocks. Coherence and phase relationships of the other five
512 legs to the anchor was compared at the determined fundamental frequency.
513 *Groundswell* uses coherence magnitude as a measure of the linear relationship
514 between two waveforms at the determined fundamental frequency, and calculates a
515 coherence magnitude threshold with the formula:

516 $$C_mag_thresh = \sqrt{1 - \alpha^{\frac{1}{(\mathrm{dof}/2-1)}}})$$

517 Where degrees of freedom (dof) = 2*R*K, in which R is the number of observations of
518 the waveforms together and K is the number of tapers. This threshold determines the
519 minimum coherence magnitude required for significant coherence between two
520 signals with α = 0.05.

521 *Preliminary incline assay*

522 Ten larvae were individually placed on custom-built platforms of varying incline (180°
523 – flat substrate, 135° – slight upwards incline, 90° – vertical wall, 45° – overhang).
524 Locomotion was filmed with an MQ022RG-CM XIMEA CMOS (Ximea GmbH, Münster,
525 Germany) camera for 1 minute at 30fps with a Thorlabs OSL1 Fiber Illuminator
526 (Thorlabs Inc, NJ, USA) with gooseneck lights at lowest intensity. Raw videos were
527 optimized for FIMTrack in Fiji with custom-written macros. Statistical analysis on mean
528 instantaneous velocity was performed as one-way ANOVA.

529 *Connective severing assay*

530 In preliminary control assays, six larvae were anesthetized on ice and sequestered
531 between 0.1mm tungsten pins ventral side up on a dissection dish. A cut was made
532 with fine microdissection scissors on the cuticle line separating A1 and A2 segments.
533 The blades were inserted at a ~45° angle to the cuticle and pulled upwards to sever
534 the connective. Sham larvae were given lateral lesions on A1. Control larvae were not
535 lesioned but anesthetized on ice for equal time. Surgeries were verified via fillet

536 microdissection post-experimentally. Larvae without clear, visible connective severing
537 were discarded from results. Behavior was filmed with the setup outlined in *Free*
538 *locomotion assay* 2 hours after surgery; raw videos were processed in Fiji and tracked
539 with FIMTrack. Statistical analysis on mean instantaneous velocity was performed as
540 a between-subjects one-way ANOVA.

541 For following incline and tunnelling experiments, surgeries were repeated on seven
542 larvae; sham animals' lateral lesions alternated between left and right sides to
543 minimize biases in turning. Different animals were used for incline and tunnelling
544 assays to avoid excessive fatigue on lesioned animals.

545 *Top-down connective severing incline assay*

546 Same methodology as *Preliminary incline assay,* excluding 90° due to short lifespans
547 of severed animals. 2 larvae (1 control and 1 severed) could not be tracked with
548 FIMTrack, thus mean velocity was obtained with wrMTrck
549 (https://www.phage.dk/plugins/wrmtrck.html) and their tracks are therefore absent in
550 Fig. 5a. Statistical analysis on mean instantaneous velocity was performed as a
551 repeated-measures ANOVA with Bonferroni corrected post-hocs.

552 *Up-close connective severing incline assay*

553 Control, sham and severed larvae were individually placed onto a walled 70mm x 3mm
554 paper platform on a custom-built rig; incline was adjusted with a micromanipulator and
555 verified with a protractor. Locomotion was filmed until the animal walked out of view
556 with a MQ042RG-CM XIMEA CMOS (Ximea GmbH, Münster, Germany) camera
557 connected with a 1"-32 C-mount (Thorlabs Inc, NJ, USA) to a Canon FR1048KWN
558 lens (Canon Inc, Tokyo, Japan). If the animal remained immobile, filming was stopped
559 at the experimenter's discretion. 180° videos were filmed at 100fps and illuminated by
560 an overhead Thorlabs M850L3 850nm light (Thorlabs Inc, NJ, USA). 45° overhang
561 trials were illuminated from the bottom with a Stemmer Imaging CCS LDL100 850nm
562 light (Stemmer Imaging Ltd, Tongham, UK) and limited to 50fps by the field of view.
563 135° and 90° were not tested due to the short lifespans of severed animals. For
564 analysis, velocity was tracked with FIMTrack; pygopod planting events and start and
565 stop frames of leg swings were manually tracked with Fiji's Manual Tracking plugin.
566 The constricted arena walls promoted exploration, therefore to effectively analyze

567 locomotor parameters and gait kinematics, walk cycles following the T3 to T1
568 sequence were extracted and stance durations above median ± 1SD were discarded
569 to filter out pause periods. Mean percentage of sequences extracted out of total
570 tracked time (including pauses) per animal were: 55.4% (control 180°), 47.2% (sham
571 180°), 34.2% (severed 180°), 28.3% (control 45°), 24.9% (sham 45°) and 26.0%
572 (severed 45°). Cycle period, stance duration and duty cycle retained their definitions
573 in *Gait characterization,* but swing duration was calculated as the time between swing
574 start and swing stop frames.

575 A pygopod plant event was defined as a visible extension of the pygopods, forming
576 almost a blunt triangular point, into the substrate, regardless of whether the abdomen
577 is in contact with the substrate. The Freedman-Diaconis rule was used in Fig. 5r, using
578 the formula: $(2*IQR) / 3\sqrt{n}$ to calculate x-axis bin length. Planting rate was used for
579 Fig. 5t to normalize for variable video lengths, calculated as number of events over
580 total tracked time. Pearson's correlations were applied for regression analyses.

581 *Tunneling assay*

582 Post-surgery animals were allowed to wake and begin walking on paper before testing.
583 A circular dish was filled with ~10mm of flour; control, sham and severed larvae were
584 individually placed and filmed with an MQ0113RG-E2 XIMEA CMOS (Ximea GmbH,
585 Münster, Germany) at 15fps under a Nikon SMZ745T dissection scope at 0.63x
586 magnification**.** Filming stopped at 2 minutes regardless of how deep larvae tunneled.
587 Body lengths at time 0s and 120s were measured in Fiji. Statistics was performed as
588 a Kruskal-Wallis test and Dunn post-hoc analysis with Bonferroni correction (given
589 non-normal data distribution).

590 **Data availability**

591 Source data is available at: 10.5281/zenodo.11520088 (analyzed files) and
592 10.17630/a97be752-0c97-42a2-ada4-745c5acff342 (raw movies).

593 **Code availability**

594 Analysis code is available at: 10.5281/zenodo.11520206.

References

1. Phillips, T. W. & Throne, J. E. Biorational Approaches to Managing Stored-Product Insects. *Annual Review of Entomology* **55**, 375–397 (2010).
2. Good, N. E. The Flour Beetles of the Genus *Tribolium*. (1936) doi:10.22004/AG.ECON.164672.
3. Mantziaris, C., Bockemühl, T. & Büschges, A. Central pattern generating networks in insect locomotion. *Dev Neurobiol* **80**, 16–30 (2020).
4. van Griethuijsen, L. I. & Trimmer, B. A. Locomotion in caterpillars. *Biol Rev Camb Philos Soc* **89**, 656–670 (2014).
5. Leiras, R., Cregg, J. M. & Kiehn, O. Brainstem Circuits for Locomotion. *Annu Rev Neurosci* **45**, 63–85 (2022).
6. Daley, M. A. Understanding the Agility of Running Birds: Sensorimotor and Mechanical Factors in Avian Bipedal Locomotion. *Integr Comp Biol* **58**, 884–893 (2018).
7. Hooper, S. L. *et al.* Neural control of unloaded leg posture and of leg swing in stick insect, cockroach, and mouse differs from that in larger animals. *J Neurosci* **29**, 4109–4119 (2009).
8. Triphan, T., Poeck, B., Neuser, K. & Strauss, R. Visual targeting of motor actions in climbing *Drosophila*. *Curr Biol* **20**, 663–668 (2010).
9. Picker, M., Colville, J. F. & Burrows, M. A cockroach that jumps. *Biol Lett* **8**, 390–392 (2012).
10. Digumarti, K. M., Trimmer, B., Conn, A. T. & Rossiter, J. Quantifying Dynamic Shapes in Soft Morphologies. *Soft Robot* **6**, 733–744 (2019).

618 11. Booth, J. H., Meek, A. T., Kronenberg, N. M., Pulver, S. R. & Gather, M. C.
619 Optical mapping of ground reaction force dynamics in freely behaving *Drosophila*
620 *melanogaster* larvae. *eLife* **12**, (2024).
621 12. Shield, S., Jericevich, R., Patel, A. & Jusufi, A. Tails, Flails, and Sails: How
622 Appendages Improve Terrestrial Maneuverability by Improving Stability.
623 *Integrative and Comparative Biology* **61**, 506–520 (2021).
624 13. Đukić, N. *et al.* Behavioural responses of Tribolium castaneum (Herbst) to
625 different types of uninfested and infested feed. *Bulletin of Entomological*
626 *Research* **110**, 550–557 (2020).
627 14. Gerken, A. R., Scully, E. D. & Campbell, J. F. Red Flour Beetle (Coleoptera:
628 Tenebrionidae) Response to Volatile Cues Varies With Strain and Behavioral
629 Assay. *Environmental Entomology* **47**, 1252–1265 (2018).
630 15. Đukić, N. *et al.* The effect of 1-pentadecene on Tribolium castaneum behaviour:
631 Repellent or attractant? *Pest Management Science* **77**, 4034–4039 (2021).
632 16. Semeao, A. A., Campbell, J. F., Whitworth, R. J. & Sloderbeck, P. E. Response of
633 Tribolium castaneum and Tribolium confusum adults to vertical black shapes and
634 its potential to improve trap capture. *Journal of Stored Products Research* **47**,
635 88–94 (2011).
636 17. Duehl, A. J., Cohnstaedt, L. W., Arbogast, R. T. & Teal, P. E. A. Evaluating Light
637 Attraction to Increase Trap Efficiency for Tribolium castaneum (Coleoptera:
638 Tenebrionidae). *Journal of Economic Entomology* **104**, 1430–1435 (2011).
639 18. Prakashini, V. Y., Srinivasan, G., Shanthi, M. & Prabakaran, K. Preference of Red
640 Flour Beetle *Tribolium castaneum* (Herbst) Towards Colour Cues. *Indian Journal*
641 *of Entomology* 445–447 (2023) doi:10.55446/IJE.2021.151.

642 19. Romero, S. A., Campbell, J. F., Nechols, J. R. & With, K. A. Movement Behavior
643 of Red Flour Beetle: Response to Habitat Cues and Patch Boundaries.
644 *Environmental Entomology* **39**, 919–929 (2010).
645 20. Schultheis, D. *et al.* A Large Scale Systemic RNAi Screen in the Red Flour Beetle
646 *Tribolium castaneum* Identifies Novel Genes Involved in Insect Muscle
647 Development. *G3 Genes|Genomes|Genetics* **9**, 1009–1026 (2019).
648 21. Devi, M. B. & Devi, N. V. Biology of rust-red flour beetle, *Tribolium castaneum*
649 (Herbst) (Tenebrionidae:Coleoptera). *Ind. Jour. of Entomol.* **77**, 81 (2015).
650 22. Dawson, P. S. Life History Strategy and Evolutionary History of *Tribolium* Flour
651 Beetles. *Evolution* **31**, 226–229 (1977).
652 23. Pai, A. *Tribolium*. in *Encyclopedia of Animal Behavior* 446–452 (Elsevier, 2010).
653 doi:10.1016/B978-0-08-045337-8.00030-9.
654 24. King, C. E. & Dawson, P. S. Population biology and the Tribolium model. *Evol.*
655 *Biol.* **5**, 133–227 (1972).
656 25. Suster, M. L. & Bate, M. Embryonic assembly of a central pattern generator
657 without sensory input. *Nature* **416**, 174–178 (2002).
658 26. Lahiri, S. *et al.* Two Alternating Motor Programs Drive Navigation in *Drosophila*
659 Larva. *PLOS ONE* **6**, e23180 (2011).
660 27. Buchanan, S. M., Kain, J. S. & De Bivort, B. L. Neuronal control of locomotor
661 handedness in *Drosophila*. *Proc. Natl. Acad. Sci. U.S.A.* **112**, 6700–6705 (2015).
662 28. Wosniack, M. E., Festa, D., Hu, N., Gjorgjieva, J. & Berni, J. Adaptation of
663 *Drosophila* larva foraging in response to changes in food resources. *Elife* **11**,
664 e75826 (2022).
665 29. Hunt, E. R. *et al.* Ants show a leftward turning bias when exploring unknown nest
666 sites. *Biol. Lett.* **10**, 20140945 (2014).

667 30. Camhi, J. M. & Johnson, E. N. High-frequency steering maneuvers mediated by
668 tactile cues: antennal wall-following in the cockroach. *Journal of Experimental*
669 *Biology* **202**, 631–643 (1999).
670 31. Soibam, B. *et al.* Open-field arena boundary is a primary object of exploration for
671 Drosophila. *Brain Behav* **2**, 97–108 (2012).
672 32. Wilson, D. M. Insect walking. *Annu Rev Entomol* **11**, 103–122 (1966).
673 33. Gustafson, G. T. & Chaboo, C. S. Ambulatory Use of Ventro-Lateral Abdominal
674 Ampullae by Larvae of *Labidomera clivicollis* (Kirby) (Coleoptera: Chrysomelidae:
675 Chrysomelinae). *cole* **63**, 357–363 (2009).
676 34. Zurek, D. B., Gorb, S. N. & Voigt, D. Locomotion and attachment of leaf beetle
677 larvae *Gastrophysa viridula* (Coleoptera, Chrysomelidae). *Interface Focus* **5**,
678 20140055 (2015).
679 35. Mulloney, B. & Smarandache-Wellmann, C. Neurobiology of the crustacean
680 swimmeret system. *Prog Neurobiol* **96**, 242–267 (2012).
681 36. Zhang, C., Guy, R. D., Mulloney, B., Zhang, Q. & Lewis, T. J. Neural mechanism
682 of optimal limb coordination in crustacean swimming. *Proc. Natl. Acad. Sci.*
683 *U.S.A.* **111**, 13840–13845 (2014).
684 37. Manton, S. M. The Evolution of Arthropodan Locomotory Mechanisms. Part 71.
685 Functional Requirements and Body Design in Colobognatha (diplopoda),
686 Together with a Comparative Account of Diplopod Burrowing Techniques, Trunk
687 Musculature and Segmentation. *Journal of the Linnean Society of London,*
688 *Zoology* **44**, 383–462 (1961).
689 38. Smolka, J., Byrne, M. J., Scholtz, C. H. & Dacke, M. A new galloping gait in an
690 insect. *Current Biology* **23**, R913–R915 (2013).

691 39. DeAngelis, B. D., Zavatone-Veth, J. A. & Clark, D. A. The manifold structure of
692 limb coordination in walking *Drosophila*. *eLife* **8**, e46409 (2019).
693 40. Graham, D. A behavioural analysis of the temporal organisation of walking
694 movements in the 1st instar and adult stick insect *(Carausius morosus)*. *J. Comp.*
695 *Physiol.* **81**, 23–52 (1972).
696 41. Bässler, U. & Büschges, A. Pattern generation for stick insect walking
697 movements—multisensory control of a locomotor program. *Brain Research*
698 *Reviews* **27**, 65–88 (1998).
699 42. Bender, J. A. *et al.* Kinematic and behavioral evidence for a distinction between
700 trotting and ambling gaits in the cockroach Blaberus discoidalis. *Journal of*
701 *Experimental Biology* **214**, 2057–2064 (2011).
702 43. Schilling, M., Hoinville, T., Schmitz, J. & Cruse, H. Walknet, a bio-inspired
703 controller for hexapod walking. *Biol Cybern* **107**, 397–419 (2013).
704 44. Ramdya, P. *et al.* Climbing favours the tripod gait over alternative faster insect
705 gaits. *Nat Commun* **8**, 14494 (2017).
706 45. Strang, K. T. & Steudel, K. Explaining the scaling of transport costs: the role of
707 stride frequency and stride length. *Journal of Zoology* **221**, 343–358 (1990).
708 46. Hooper, S. L. Body size and the neural control of movement. *Current Biology* **22**,
709 R318–R322 (2012).
710 47. Granatosky, M. C. & McElroy, E. J. Stride frequency or length? A phylogenetic
711 approach to understand how animals regulate locomotor speed. *J Exp Biol* **225**,
712 jeb243231 (2022).
713 48. Hunnekuhl, V. S., Siemanowski, J., Farnworth, M. S., He, B. & Bucher, G.
714 Immunohistochemistry and Fluorescent Whole Mount RNA In Situ Hybridization
715 in Larval and Adult Brains of *Tribolium*. *Methods Mol Biol* **2047**, 233–251 (2020).

716 49. Farnworth, M. S., Bucher, G. & Hartenstein, V. An atlas of the developing
717 *Tribolium castaneum* brain reveals conservation in anatomy and divergence in
718 timing to *Drosophila melanogaster*. *Journal of Comparative Neurology* **530**,
719 2335–2371 (2022).
720 50. Richter, S. *et al.* Invertebrate neurophylogeny: suggested terms and definitions
721 for a neuroanatomical glossary. *Front Zool* **7**, 29 (2010).
722 51. Mayer, G. *et al.* Selective neuronal staining in tardigrades and onychophorans
723 provides insights into the evolution of segmental ganglia in panarthropods. *BMC*
724 *Evol Biol* **13**, 230 (2013).
725 52. Nirody, J. A. Universal Features in Panarthropod Inter-Limb Coordination during
726 Forward Walking. *Integrative and Comparative Biology* **61**, 710–722 (2021).
727 53. Truman, J. W. & Bate, M. Spatial and temporal patterns of neurogenesis in the
728 central nervous system of Drosophila melanogaster. *Dev Biol* **125**, 145–157
729 (1988).
730 54. Jamnback, H. & Frempong-Boadu, J. Testing blackfly larvicides in the laboratory
731 and in streams. *Bull World Health Organ* **34**, 405–421 (1966).
732 55. Amante, M., Russo, A., Schöller, M. & Steidle, J. L. M. Olfactory host location and
733 host preference of Holepyris sylvanidis (Brèthes) (Hymenoptera: Bethylidae), a
734 parasitoid of Tribolium confusum Jacquelin du Val and T. castaneum (Herbst)
735 (Coleoptera: Tenebrionidae). *Journal of Stored Products Research* **78**, 105–109
736 (2018).
737 56. Zurek, A. J. *et al.* Quantification of anthropogenic impact on groundwater-
738 dependent terrestrial ecosystem using geochemical and isotope tools combined
739 with 3-D flow and transport modelling. *Hydrology and Earth System Sciences* **19**,
740 1015–1033 (2015).

741 57. Schmitt-Engel, C. *et al.* The iBeetle large-scale RNAi screen reveals gene
742 functions for insect development and physiology. *Nat Commun* **6**, 7822 (2015).
743 58. Hakeemi, M. S. *et al.* Screens in fly and beetle reveal vastly divergent gene sets
744 required for developmental processes. *BMC Biology* **20**, 38 (2022).
745 59. Richards, S. *et al.* The genome of the model beetle and pest *Tribolium*
746 *castaneum*. *Nature* **452**, 949–955 (2008).
747 60. Schinko, J. B. *et al.* Functionality of the GAL4/UAS system in *Tribolium* requires
748 the use of endogenous core promoters. *BMC Developmental Biology* **10**, 53
749 (2010).
750 61. Gilles, A. F., Schinko, J. B. & Averof, M. Efficient CRISPR-mediated gene
751 targeting and transgene replacement in the beetle Tribolium castaneum.
752 *Development* **142**, 2832–2839 (2015).
753 62. Adrianos, S., Lorenzen, M. & Oppert, B. Metabolic pathway interruption:
754 CRISPR/Cas9-mediated knockout of tryptophan 2,3-dioxygenase in Tribolium
755 castaneum. *J Insect Physiol* **107**, 104–109 (2018).
756 63. Tomoyasu, Y. *et al.* Exploring systemic RNA interference in insects: a genome-
757 wide survey for RNAi genes in Tribolium. *Genome Biology* **9**, R10 (2008).
758 64. Naseem, M. T. *et al.* NHA1 is a cation/proton antiporter essential for the water-
759 conserving functions of the rectal complex in Tribolium castaneum. *Proceedings*
760 *of the National Academy of Sciences* **120**, e2217084120 (2023).
761 65. He, B. *et al.* An ancestral apical brain region contributes to the central complex
762 under the control of foxQ2 in the beetle Tribolium. *eLife* **8**, e49065 (2019).
763 66. Garcia-Perez, N. C., Bucher, G. & Buescher, M. Shaking hands is a
764 homeodomain transcription factor that controls axon outgrowth of central

complex neurons in the insect model Tribolium. *Development* **148**, dev199368 (2021).

67. Farnworth, M. S., Bucher, G. & Hartenstein, V. An atlas of the developing Tribolium castaneum brain reveals conservation in anatomy and divergence in timing to Drosophila melanogaster. *J Comp Neurol* 10.1002/cne.25335 (2022) doi:10.1002/cne.25335.
68. Schindelin, J. *et al.* Fiji: an open-source platform for biological-image analysis. *Nat Methods* **9**, 676–682 (2012).
69. Risse, B., Otto, N., Berh, D., Jiang, X. & Klämbt, C. FIM Imaging and FIMtrack: Two New Tools Allowing High-throughput and Cost Effective Locomotion Analysis. *J Vis Exp* 52207 (2014) doi:10.3791/52207.
70. Xu Ying, B., Zwart, M.F. and Pulver, S.R. (2024) 'Context-dependent coordination of movement in *Tribolium castaneum* larvae'. Dataset. University of St Andrews Research Portal. https://doi.org/10.17630/a97be752-0c97-42a2-ada4-745c5acff342

End Notes

Acknowledgements

This project was supported by the Institute of Behavioural and Neural Sciences Undergraduate Research Assistant Scheme at the University of St Andrews. We thank Barry Denholm for providing *Tribolium* stocks and advice early in the project, Adam Taylor from Janelia Research Campus for *Groundswell*, Balwant Singh for help building the up-close incline rig, and members of the Pulver and Zwart Labs for constant support.

Author contributions

B.X.Y., M.F.Z. and S.R.P. conceived experiments; B.X.Y. reared animals, performed all experiments and analyzed data; M.F.Z. and B.X.Y. analyzed gait data; M.F.Z. and

S.R.P. performed surgeries; B.X.Y. prepared figures and drafted manuscript; S.R.P. and M.F.Z. revised manuscript; S.R.P and M.F.Z. supervised the project.

Conflicts of interest

The authors declare no conflicts of interest.